J Neuropathol Exp Neurol
Vol. 77, No. 9, September 2018, pp. 782–792
doi: 10.1093/jnen/nly054

ORIGINAL ARTICLE

Intensity Specific Repetitive Mild Traumatic Brain Injury Evokes an Exacerbated Burden of Neocortical Axonal Injury

Yasuaki Ogino, MD, PhD, Michal Vascak, BS, and John T. Povlishock, PhD

Abstract

Mild traumatic brain injury (mTBI) has been linked to enduring neurological damage following repetitive injury. Previously, we reported that intensity-specific, repetitive mTBI exacerbated microvascular and axonal damage in brainstem. For a more rigorous and global assessment, we assessed the burden of neocortical diffuse axonal injury (DAI) evoked by repetitive mTBI. Mice were subjected to mild central fluid percussion injuries at 1.4 and 1.6 atm with or without repetitive insult at a 3-hour interval and killed at 24 hours postinjury. Neocortical DAI within layer V was quantitatively assessed by double-labeling p-c-Jun and NeuN to identify both the axotomized and total neuronal population. Both confocal and electron microscopic findings revealed no apparent evidence of neuronal death. Repetitive mTBI of 1.6 atm group, but not of 1.4 atm group, demonstrated a significantly higher proportion of axotomized neurons. These results demonstrate that different intensities of mTBI induced different burdens of DAI after repetitive insult. Interestingly, the parallel loss of the righting reflex reflected differences in injury intensity, yet the duration of this reflex was not elongated by the repetitive insult. These data highlight some of the complex issues surrounding repetitive mTBI and its associated morbidity, mandating the need for continued exploration.

Key Words: Diffuse axonal injury, Layer V neurons, Mild traumatic brain injury, Neocortex, Repetitive traumatic brain injury.

INTRODUCTION

Over the last decade, there has been dramatically increased recognition of the potential damaging consequences of mild traumatic brain injury (mTBI), leading to its increased investigation in both the clinical and laboratory settings. The global incidence of mTBI is substantial, currently ∼600 cases per 100 000 individuals, with recognition that mTBI represents 70%–90% of the overall TBI hospital admissions (1). Not only is there increased interest in the incidence of mTBI and its pathophysiology and potential morbidity, but so, too, is there increased interest in its potential exacerbation following repetitive mild injuries, with some groups suggesting that such repetitive injuries can progress to a constellation of neurodegenerative change (2–5), leading to the condition of chronic traumatic encephalopathy (6). Although these neurodegenerative changes remain a matter of controversy, there is compelling evidence, particularly from the laboratory front, that repetitive mild injuries can cause an increased burden of CNS damage, with laboratory evidence showing that repetitive injury can result in exacerbated metabolic, vascular, axonal, and neuronal changes (7–13). While there is no consensus on this issue, there is emerging thought that not all repetitive injuries are the same, with the suggestion that the more damaging consequences of repetitive injury are associated not only with the duration or interval between the repetitive insults but also, the initial loading conditions associated with the injury itself. This has been demonstrated by our own group assessing pial microvascular change as well as local axonal injury (14). Because of the complexities of these studies, the analysis of axonal injury was confined to the brainstem, with no consideration of more global axonal change, which may be more biologically significant in addition to being more clinically relevant. Moreover, since these studies relied on the use of amyloid precursor protein immunocytochemistry to assess the burden of axonal injury, the limitations of this approach could underestimate the total burden of traumatically induced axonal change (15). Accordingly, it seemed both reasonable and rational to revisit the issue of repetitive mild injury following different intensities of mild injury to allow for a more global assessment of the burden of axonal injury within specific neocortical domains.

In the current study, we address these issues by assessing the widespread neocortical response to repetitive mild brain injury of differing intensity, examining the potential for diffuse axonal injury (DAI) via a recently well-characterized marker of DAI, phosphorylated c-Jun (p-c-Jun). The benefits of this marker reside in the fact that it is confined to the nuclei of only those neuronal soma undergoing traumatically induced axonal injury, a finding confirmed in our lab as well as that of others (16–19), while also permitting the use of double-labeling with a pan-neuronal marker, NeuN, to confirm its neuronal localization and density. Further, since p-c-Jun is

From the Department of Anatomy and Neurobiology, Virginia Commonwealth University, Richmond, Virginia (YO, MV, JTP)
Send correspondence to: John T. Povlishock, PhD, Department of Anatomy and Neurobiology, Virginia Commonwealth University, PO Box 980709, Richmond, VA 23298-0709; E-mail: john.povlishock@vcuhealth.org
This research was supported by National Institute of Health (NIH) Grants NS077675. Also, the microscopy performed at the VCU Department of Anatomy and Neurobiology Microscopy Facility, was supported, in part, by funding from NIH-NINDS Center Core Grants (5P30NS047463), and by funding from NIH-NCI Cancer Center Support Grants (P30 CA016059).
The authors have no duality or conflicts of interest to declare.

also a robust marker that persists for weeks post TBI (16), its benefits were considered significant. These studies were complemental by ultrastructural studies to confirm tracer specificity as well as brain tissue integrity and the absence of overt neuronal death. Collectively, these studies reaffirmed the damaging consequences of repetitive mild brain injury, while also demonstrating that the initial loading conditions/injury severity are major determinants of the overall increased damage associated with the repetitive insult.

MATERIALS AND METHODS

All protocols were approved by Institutional Animal Care and Use Committee of Virginia Commonwealth University.

Animals

Adult male mice C57BL/6J (8–11 weeks) were obtained directly from Jackson Laboratory (Bar Harbor, ME) or bred and maintained in house. Out-sourced animals were kept in house for 24 hours to habituate prior to experimentation. Animals were housed under a 12-hour light/12-hour dark cycle with free access to food and water. A total of 20 animals were subjected for the experimentations following group assignment described below.

Surgical Preparation and Physiological Assessments During Surgery

Animals were subjected to surgical preparation for central fluid percussion injury (cFPI) as previously described (16). Briefly, 3-mm-diameter craniectomy along the sagittal suture midway between bregma and lambda was employed, and a 20-gauge luer-lock hub was placed and stabilized on the skull over the craniectomy site using cyanoacrylate and dental acrylic. All surgical procedures were performed sterilely under anesthesia initially induced via inspiration of 4% isoflurane in 100% oxygen in anesthesia chamber. This was then maintained with flow of 2% isoflurane in 100% oxygen from a nose cone with the mouse fitted in a stereotaxic frame (David Kopf Instruments, Tujunga, CA). An adequate plane of anesthesia was ensured by checking the absence of toe pinch response.

Thermostatically controlled heating pad with a rectal temperature sensor (Harvard Apparatus, Holliston, MA) was used to maintain body temperature at 37°C, and thigh-clump pulse oximeter sensor (MouseOx; STARR Life Sciences, Oakmont, PA) was used to monitor heart rate, respiratory ratio, and arterial blood oxygenation (SpO_2). After surgery, animals were placed in a warmed cage until their full recovery from anesthesia.

Experimental Design

As summarized in Figure 1, animals were assigned into 4 different groups of mTBI, which included a lower intensity single mild injury (LS) group, a lower intensity repetitive mild injury (LR) group, a higher intensity single mild injury (HS) group, and a higher intensity repetitive mild injury (HR) group. Those groups were defined by the different mild injury intensities employed, which targeted at 1.4 atm for low intensity mTBI and at 1.6 atm for a higher intensity mTBI, and by the numbers of injuries. The injury intensities were chosen based on our previous experience with this model of mTBI (16, 17, 20). Neither the lower nor higher intensity injury groups were randomized; however, randomization was employed in the conduct of the singular versus the repetitive injuries. In the repetitive injury groups, experimental mTBI was produced twice over a 3-hour interval between injuries, while the single injury groups employed an initial mTBI followed by sham injury at 3 hours after the initial injury. Prior to any experimental mTBI, the animals were fully anesthetized in the same fashion. Experimental mTBI was induced via FPI device (Custom Design and Fabrication, Virginia Commonwealth University, Richmond, VA) connected with luer lock hub installed on the animal's skull using a connector tube filled with sterile saline. Details of the device are described elsewhere (21). The pendulum position of the device was calibrated to target 1.4 atm for the lowest intensity mild cFPI and at 1.6 atm for the higher intensity mild cFPI. The actual intensity of the pressure wave impacting the animal's dural surface was measured by a transducer at the end of device's cylinder and displayed on an oscilloscope (Tektronix TDS 210; Tektronix Inc., Beaverton, OR). For sham injury, identical procedures were used except for the pendulum's release.

Postinjury Behavioral Assessments

After cFPI, the animals were closely monitored until recovery of righting reflex, then they were transferred to a warmed cage. Durations of loss of righting reflex time (LORR), a widely used measure for assessing the loss of consciousness in animals (22), were recorded at each time after the first injury (first LORR) and the second injury (second LORR). After the second mTBI, the skin around the injury site was sutured and animals were returned to the vivarium. Since the assessment of the LORR was always performed immediately following the induction of the traumatic event by the same examiner who initiated cFPI, the blinding was not possible.

Perfusion and Tissue Preparation

Twenty-four hours after the second mTBI, or alternatively 27 hours after the first mTBI in the single injury groups, animals were killed with an intraperitoneally injected overdose of pentobarbital and were then subjected to transcardial perfusion with heparinized saline, followed by 4% paraformaldehyde in Millonig's buffer pH 7.4. For animals for electron microscope (EM) study, 4% paraformaldehyde with 0.2% glutaraldehyde in Millonig's buffer pH 7.4 was used as a fixative solution. After perfusion, the occipital and parietal bone were removed, then brain was removed from the skull and immersed in the same fixative solution overnight, followed by replacement with Millonig's buffer in 4°C.

Coronally dissected brains at the optic chiasm and the midbrain were embedded in agarose and then were cut using a vibratome (Leica VT1000S; Leica Biosystems, Nussloch,

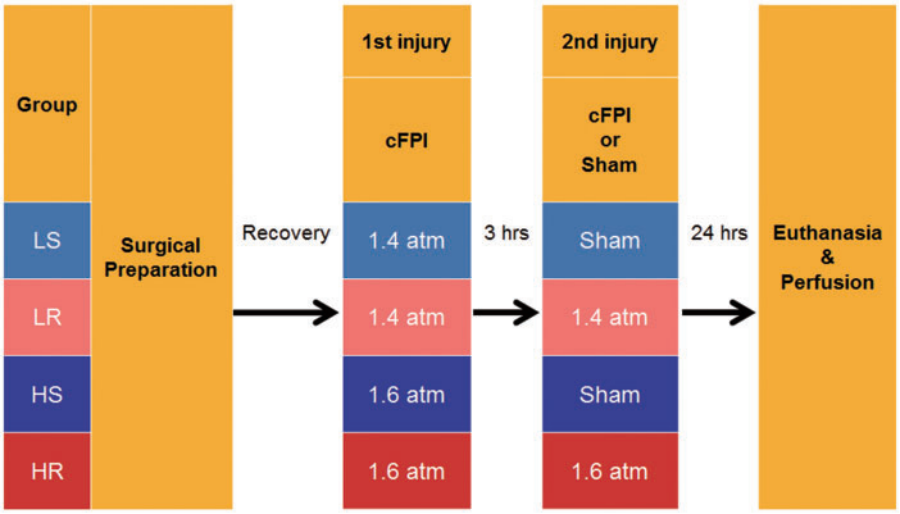

FIGURE 1. Group assignment and experimental paradigm. Animals were assigned to 4 experimental groups defined by the following 2 factors: Injury intensity (low or high), and the number of injuries (single or repetitive). Target intensities of injury were 1.4 atm for the lower intensity and 1.6 atm for the higher intensity. After postsurgical recovery, all animals were subjected to central fluid percussion injury (cFPI) at the target intensity. Three hours later, the second cFPI at the same intensity for the repetitive injury groups, or sham injury for the single injury groups, was initiated. Animals were killed and perfused at 24 hours after the second injury for immunocytochemical assessments. LS: lower intensity single mild injury, LR: lower intensity repetitive mild injury, HS: higher intensity single mild injury, HR: higher intensity repetitive mild injury.

Germany) to obtain 40-μm-thick, serial floating slices directly below the craniectomy site (from -0.58 mm to -2.5 mm posterior to bregma), in which our mTBI model generates DAI within a well-defined region of neocortical gray matter containing the primary somatosensory cortex (S1) (16, 17). Sections were collected in 24-well plate and stored in Millonig's buffer pH 7.4 at 4°C. The caudal 24 sections of total 48 sections were used for analyses, dividing them into 6 sets of sections, containing 4 sections spaced 240 μm apart. One set was randomly selected from the 6 sets for use in the p-c-Jun/NeuN immunohistochemical staining.

Immunocytochemical Approaches

As detailed below, multiple antibodies were employed in double labeling strategies to evaluate the burden of axonal injury within the total neuron populations. Samples from all animals were stained in the same session, employing randomization and blinding to preclude animal identity for the origin of the tissue sample. The antibody for p-c-Jun, which identified the axotomized neuronal soma (16–19), was used for the assessment of the burden of axonal injury in the combination with the antibody for NeuN to achieve the evaluation of the total neuron population assessed.

Immunohistochemistry

Ten percent normal goat serum and 2% fish skin gelatin in TBS was used as blocking buffer, and 1% normal goat serum and 1% fish skin gelatin in TBS was used as dilution buffer in following procedures. Free-floating sections were washed with TBS, which was then replaced by 10 mM sodium citrate buffer pH8.5 with 0.05% Tween 20. The plates were placed in heated water bath at a temperature of 80°C for 10 minutes to retrieve antigen epitopes, followed by gradual cooling in room temperature. Tissues were then incubated in blocking buffer for 1 hour to block potential sites for unspecific reactions with primary antibodies. After blocking buffer was removed, tissues were placed in primary antibody solution, which consists of primary antibodies in dilution buffer, and incubated overnight in a refrigerator controlled at 4°C temperature. Then tissues were washed with dilution buffer and incubated in secondary antibody solution, which consists of secondary antibodies in dilution buffer, for 2 hours. Tissues were again washed 3 times each with dilution buffer and TBS. Tissues were placed on plain glass slides individually and sealed using mounting medium.

Primary antibodies labeling the following antigens were utilized in following dilutions; p-c-Jun (Ser63; anti-rabbit polyclonal, #9261, 1:100; Cell Signaling, Danvers, MA), NeuN (anti-mouse IgG1 clone A60, MAB377, 1:500; Millipore, Billerica, MA). Fluorophore-conjugated secondary antibodies were utilized in dilutions as follows; goat-derived anti-rabbit-IgG Alexa A568 (1:500; Thermo Fisher Scientific, Waltham, MA), goat-derived anti-mouse-IgG1 Alexa A488 (1:500; Thermo Fisher Scientific). Vectashild (hard-set; Vector Laboratories, Burlingame, CA) was used as a mounting medium.

Confocal Microscopy

Image acquisition was performed using laser-scanning confocal microscope LSM710 (Carl-Zeiss Microscopy, Jena, Germany) with 20× objective lens (Plan-Apochromat 20×/0.8 M27). Image acquisition was performed in random order

and in blinded fashion. All images were finally saved as tag image format (TIFF).

As noted, antibodies were chosen for their unique properties in identifying neurons that have sustained axonal injury (p-c-Jun) or alternatively identifying the entire neuronal populations (NeuN). NeuN provided an excellent map of the neocortex and specifically layer V to determine identical region of interest (ROI) for the p-c-Jun analysis. In this approach, the field of view was centered initially over the S1 along the dorsolateral edge of the hippocampus using 10× objectives (EC Plan-Neofluar 10×/0.30 M27). The field of view was then rotated until it was orthogonal to the subcortical white matter and centered midway between upper and lower limit of neocortical layer V. Images were acquired using 20× objectives after readjustment to maintain centering. The pinhole was optimized at 1.0 ± 0.3 airy units for green and red channel (488 Argon, 561 DPSS). Gain and offset were adjusted for optimal single range with the lowest possible power for each channel to avoid crosstalk. For layer V to be targeted in this study, based on our previous published experiences with this model, 2 adjacent areas with the sizes of 424.94 μm × 207.06 μm were captured and the images were processed by ZEN 2.1 (black edition) imaging software (Carl-Zeiss Microscopy) to generate 2 × 1 tiled image with the final size of 828.85 × 207.06 μm after exclusion of any overlap. Within optical slice thickness, the center plane and the other 2 planes 3 μm apart from the center were captured and a composite image was obtained using "maximum intensity projection" function of the software to achieve good separation of NeuN positive area between different neurons. Finally, 4 sections per 1 animal were used and 2 sides of each section were captured, yielding a total of 8 tiled, composite images obtained from each animal.

Quantitative Image Analysis

Quantitative image analysis was performed using ImageJ software (National Institutes of Health, Bethesda, MD), with the investigator blinded from the identity of each image. Prior to experimental analysis, macro scripts were built and optimized for each channel using a pilot set of images selected from the experimental image set. Macros were designed to selectively extract positive signal of the target markers and to convert the original images to binary image representing the distribution of the reactive soma automatically. The macro scripts were applied to image stacks of each channel, and then stacks of binary images were obtained. Using "Analyze Particles" or "Find Maxima" function, numbers of positive neuronal soma were counted automatically. Size threshold of 30–300 μm^2 was applied to the images of p-c-Jun. Images which represent colocalization of p-c-Jun and NeuN were finally obtained by the calculation using "Image Calculator" function, and the colocalization were counted using "Analyze Particles" function.

Tissue Preparation for Electron Microscopy

Consistent with previous reports form our laboratory (16, 17, 23), we employed antibodies to p-c-Jun that could be followed at the transmission EM level to confirm the nuclear location of the antibody, while also confirming that this nuclear reactivity was consistently localized to neurons that had sustained axonal injury. The EM analysis provided further benefit in that it allowed the ready assessment of the structural integrity of the somatosensory cortex in terms of its neuronal, glial, and vascular components. To this end, tissue samples adjacent to those processed for confocal microscopy or alternatively harvested from additional dedicated population of mice (perfused as described above) were randomly selected from all animal groups. The tissues were then postfixed in 4% paraformaldehyde and 0.2% glutaraldehyde for 24 hours. The sections were then rinsed 4 times (10 minutes) in TBS and endogenous peroxidase activity was blocked with 0.5% hydrogen peroxide for 30 minutes. The tissue was then processed using a temperature control antigen retrieval approach as described by our laboratory (24). The tissue was then incubated overnight in a 1:100 dilution of the p-c-Jun antibody. Next the sections were incubated for 1 hour in biotinylated goat anti-rabbit secondary antibody (Vector Laboratories) and diluted at 1:200 in 1% NGS in PBS, followed for 1 hour in a 1:200 dilution of n avidin-horseradish peroxidase complex (ABC Standard Elite Kit; Vector laboratories). The reaction product was visualized with 0.05% diaminobenzidine, 0.01% hydrogen peroxide, and 0.3% imidazole in 0.1 M phosphate buffer for 20 minutes. Next the sections were osmicated, dehydrated and placed in medcast resin (Ted Pella, Inc., Redding, CA) and then sandwiched in medcast resin between 2 plastic slides and allowed to cure in an oven for 24 hours. The embedded tissue on the slides was then scanned on a light microscope to identify the somatosensory cortex and any reaction product visible therein. With the identification of reactive neocortical neurons these areas were then cut from the embedded tissue and mounted on plastic studs. Thick sections were then cut to more precisely determine the regions of interest. Using an ultramicrotome, 700-nm serial sections were cut and picked up onto Formvar-coated slotted grids that were stained with uranyl acetate and lead citrate. Ultrastructural analysis was performed a JEOL JEM-1400 Plus transmission electron microscope (JEOL Ltd., Tokyo, Japan), equipped with a Gatan UltraScan camera (Gatan, Inc., Pleasanton, CA).

Statistical Analysis

Eight data sets from each animal were collected and combined, considering each individual animal to be a statistical unit. Normality of distribution for continuous data was assessed by Shapiro-Wilk test. Statistical analysis for parametric data sets was performed as follows: Homogeneity of variance between different groups was assessed by Brown-Forsythe test, comparisons of animal's background data between the groups were assessed by one-way analysis of variance (ANOVA), pairwise comparisons of the means between groups were assessed by Tukey's honestly significant difference (HSD) test, and comparisons of the means between the groups by 2 different explanatory variables were assessed by two-way ANOVA. The LORR change between the first injury and the second injury was assessed by paired t test for equal variance data set, while the Welch's t test was used for

TABLE. Physical and Physiological Data

Variables	LS (n = 5)	LR (n = 5)	HS (n = 5)	HR (n = 4)	p Value
Age (days)	68 ± 4	69 ± 3	64 ± 2	63 ± 2	0.440 (a)
Body weight (g)	23.0 ± 0.8	22.6 ± 0.6	24.2 ± 1.0	24.5 ± 1.0	0.373 (a)
Physiological parameters during surgery					
Time under anesthesia (min)	63.0 ± 0.8	57.3 ± 3.8	59.3 ± 2.5	70.2 ± 3.5	0.037 (a)
Heart rate (bpm)	497 ± 20	512 ± 15	517 ± 33	509 ± 18	0.933 (a)
Respiratory rate (/min)	94 ± 6	85 ± 4	66 ± 7	62 ± 7	0.006 (a)
SpO_2 (%)	97.7 ± 0.2	97.9 ± 0.2	97.3 ± 0.4	97.2 ± 0.2	0.346 (b)
Time from the completion of surgery to the first injury (min)	104.4 ± 13.8	111.8 ± 18.3	94.2 ± 14.9	144.5 ± 11.8	0.703 (a)
Intensity of injury (atm)					
First injury	1.43 ± 0.02	1.39 ± 0.02	1.59 ± 0.01	1.58 ± 0.02	
Second injury	(Sham)	1.44 ± 0.04	(Sham)	1.62 ± 0.02	

All values are presented as "Mean ± SEM." (a); One-way analysis of variance, (b); Kruskal-Wallis.
SEM; standard error of the means, SpO_2; arterial blood oxygenation.
LS; lower intensity single mild injury, LR; lower intensity repetitive mild injury, HS; higher intensity single mild injury, HR; higher intensity repetitive mild injury.

unequal variance data set. For nonparametric data sets, 2 group comparison of the length of LORR was assessed by one-sided Mann-Whitney *U* test, comparisons of the means between multiple groups were assessed by Kruskal-Wallis test, and pairwise comparisons of the means between groups were assessed by Steel-Dwass test. For proportional data, chi-square test was performed for comparisons between multiple groups followed by posthoc, pairwise chi-square test with Holm's correction for multiplicity. Odds ratio (OR) was calculated to evaluate the effect size for proportional data. Data were summarized as mean ± SEM. Cohen's *d* with Hedges' correction, *r*, or η^2 was calculated to evaluate effect size for each comparison. All analyses were two-sided, with only one exception described above. p values below 0.05 were considered as significant. Statistical analysis was performed using R software (version 3.4.1) with the following add on packages: "car," "effsize," "exactRankTests," "NSM3," "Rmisc," "sjstats," "vcd," "ggplot2."

RESULTS

Animal Assignment

Five animals were initially assigned to each group. However, upon processing, one animal of HR group revealed hemorrhage within the medullospinal junction, a finding inconsistent with mild injury (21). Accordingly, this animal was excluded from analyses, resulting in 4 animals in the HR group, with 5 animals each for the other groups.

Animal Physiological Data (Table)

There were no significant differences between groups in either age (LS; 68 ± 4, LR; 69 ± 3, HS; 64 ± 2, HR; 63 ± 2 days) or body weight (LS; 23.0 ± 0.8, LR; 22.6 ± 0.6, HS; 24.2 ± 1.0, HR; 24.5 ± 1.0 g) at the time of the surgery. Further, those variables related to heart rate (LS; 497 ± 20, LR; 512 ± 15, HS; 517 ± 33, HR; 509 ± 18 bpm), as well as the SpO_2 (LS; 97.7 ± 0.2, LR; 97.9 ± 0.2, HS; 97.3 ± 0.4, HR; 97.2 ± 0.2%) were not significantly different. However, the duration of anesthesia (LS; 63.0 ± 0.8, LR; 57.3 ± 3.8, HS; 59.3 ± 2.5, HR; 70.2 ± 3.5 minutes, p = 0.037), as well as the respiratory rate (LS; 94 ± 6, LR; 85 ± 4, HS; 66 ± 7, HR; 62 ± 7/minutes, p = 0.006) were significantly different between groups. The time from the termination of anesthesia to the induction of the first injury was not significantly different between the groups (LS; 104.4 ± 13.8, LR; 111.8 ± 18.3, HS; 94.2 ± 14.9, HR; 144.5 ± 11.8 minutes).

Injury Intensity and the LORR

The injury intensities to which the animals were subjected, except those undergoing sham injuries, were 1.42 ± 0.02 atm for lower intensity mild injuries (Table; first injury for LS; 1.43 ± 0.02, first injury for LR; 1.39 ± 0.02, second injury for LR; 1.44 ± 0.04 atm) and 1.59 ± 0.01 atm for higher intensity mild injuries (first injury for HS; 1.59 ± 0.01, first injury for HR; 1.58 ± 0.02, second injury for HR; 1.62 ± 0.02). Collectively, there was no significant difference in the injury intensities imposed on the animals between the groups and the first and second injuries which targeted the same magnitude of injury severity.

In relation to the LORR, the first LORR was significantly different between the lower intensity mild injury group (L), which represented the combination of the LS and LR groups, and the higher intensity mild injury group (H), which represented the combination of the HS and HR groups (Fig. 2A; L; n = 10, 261 ± 17 seconds, higher intensity mild injury; n = 9, 343 ± 33 seconds, $r = 0.73$, p = 0.027). Pairwise comparisons between groups showed no significant differences in the first LORR (LS; 279 ± 31, LR; 243 ± 11, HS; 333 ± 35, HR; 354 ± 67 seconds. HR vs LS; $d = 0.65$, HR vs LR; $d = 1.09$, HR vs HS; $d = 0.17$, HS vs LS; $d = 0.67$, HS vs LR; $d = 1.42$, LR vs LS; $d = 0.63$). The injury intensity demonstrated a significant effect on the first LORR (the number of injuries; $\eta^2 < 0.01$, injury intensities; $\eta^2 = 0.23$, p = 0.048, and their interaction; $\eta^2 = 0.03$). The second LORR, in either HR and LR groups showed a significant difference compared with both HS and LS groups, respectively (LS; 87 ± 23, LR;

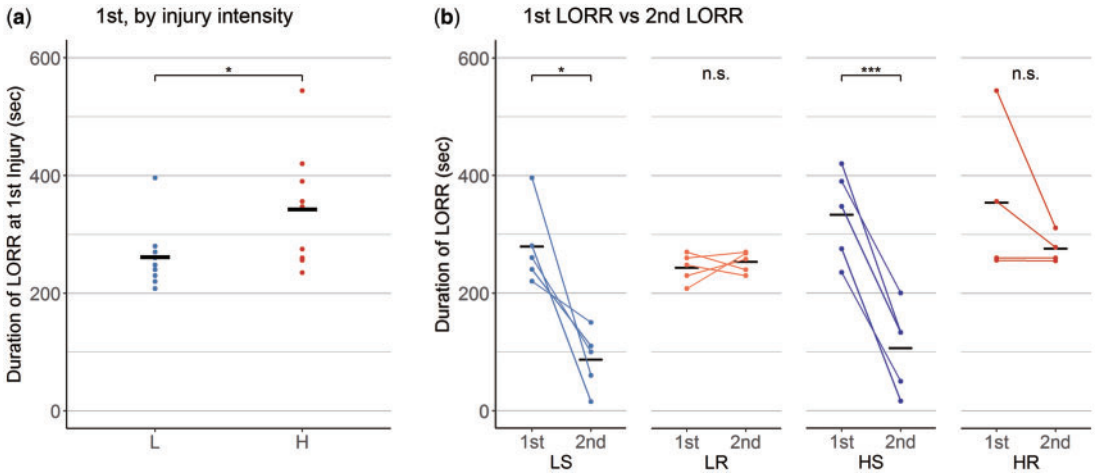

FIGURE 2. Duration of loss of righting reflex. **(A)** Comparison of loss of righting reflex time after the first injury (first LORR) between the 2 different injury intensities. In this analysis, the L group represents the lower intensity mild injury groups, which consists of both the LS and the LR groups, and the H group represents the higher intensity mild injury groups, which consists of both the HS and the HR groups. The first LORR showed a significant difference between L and H groups, suggesting injury intensity was reflected on the LORR. **(B)** Comparison of the first LORR and the second LORR of in each experimental group. Note that the second LORR in the LS and HS groups were comparable to that observed after sham injuries. The LR and HR groups, both of which were employed mild injuries at the same intensity twice, did not demonstrated significant difference between the first and the second LORRs, suggesting that the second insult did not alter the second LORR. Pairwise comparisons of the first LORR did not show significant difference between groups. **(A)** One-sided Mann-Whitney *U* test. **(B)** Paired *t* test for the LS, LR, and HS groups, and Welch *t* test for HR group. *$p < 0.05$, **$p < 0.01$, ***$p < 0.001$. LS; lower intensity single mild injury, LR; lower intensity repetitive mild injury, HS; higher intensity single mild injury, HR; higher intensity repetitive mild injury.

253 ± 8, HS; 106 ± 33, HR; 276 ± 13 seconds. HR vs LS; $d = 3.97$, $p < 0.001$, HR vs LR; $d = 0.95$, HR vs HS; $d = 2.60$, $p < 0.001$, HS vs LS; $d = 0.28$, HS vs LR; $d = 2.49$, $p = 0.001$, LR vs LS; $d = 3.91$, $p < 0.001$); however, it is of note that the second LORR in the LS and HS groups mirrored sham injury. The number of injuries, but not the injury intensity, demonstrated a significant effect on the second LORR (the number of injuries; $\eta^2 = 0.78$, $p < 0.001$, injury intensity; $\eta^2 = 0.01$, and their interaction; $\eta^2 < 0.01$). In LR and HR groups, the LORR did not show significant difference between the first LORR and the second LORR (Fig. 2B; LR; $d = 0.42$, HR; $d = 0.70$). LS and HS groups showed significantly different LORR between the first and the second (e.g. the LORR after sham injury; Fig. 2B; LS; $d = 2.85$, $p = 0.016$, HS: $d = 2.72$, $p < 0.001$).

General Histological Observations

Overall histological findings were consistent with the previous observations with cFPI model of mild injury (16, 17, 20, 21), with an exception of the one excluded animal that demonstrated more severe injury as noted above. The dorsal neocortex underneath the craniectomy site did not show any evidence of contusion or cavitation. The brain parenchyma was devoid of overt hemorrhage, with only occasional isolated petechial hemorrhage in subcortical layer or corpus callosum. Focal subarachnoid hemorrhage was also occasionally observed but was limited to the dorsal convexity incident to the site of injury and did not involve the entire subarachnoid compartment. Such minimal changes not involving the brain parenchyma were more frequently observed in the higher intensity mild injuries or the repetitively injured animals. There was no evidence of trauma-induced ventricular enlargement. Routine EM, as further detailed below, provided additional and substantial evidence of the mild nature of TBI. Other than the presence of scattered axonal damage, all the tissue sections analyzed appeared unremarkable, with no evidence of overt cellular or subcellular change (Fig. 3A). Other than the finding of axonal swellings and disconnection, the related brain parenchyma revealed normal ultrastructural detail, with the finding of intact neuronal somata and their dendritic appendages, interspersed with normal appearing synaptic profiles. The extracellular space appeared normal and the related microvessels showed no evidence of endothelial, pericytic or basal laminar damage. Collectively, these ultrastructural details supported the characterization of these injuries as mild.

Electron Microscopic Observations

In addition to the above baseline data described above, the ultrastructural analyses provided compelling evidence that the nuclear p-c-Jun reaction product was confined only to the nuclei of those neurons that had sustained axonal injury under different loading conditions (Fig. 4). In all tissues other than the shams, the p-c-Jun reaction product was found only in the nuclei of layer V neurons with no evidence of glial or microvascular uptake. Further, when these same neurons with reactive nuclei were followed by serial section analyses, they were always linked to the occurrence of DAI, which was most readily confirmed in the perisomatic regions. Accordingly, as in previous communications, these ultrastructural analyses provide further direct evidence that the p-c-Jun is an exclusive

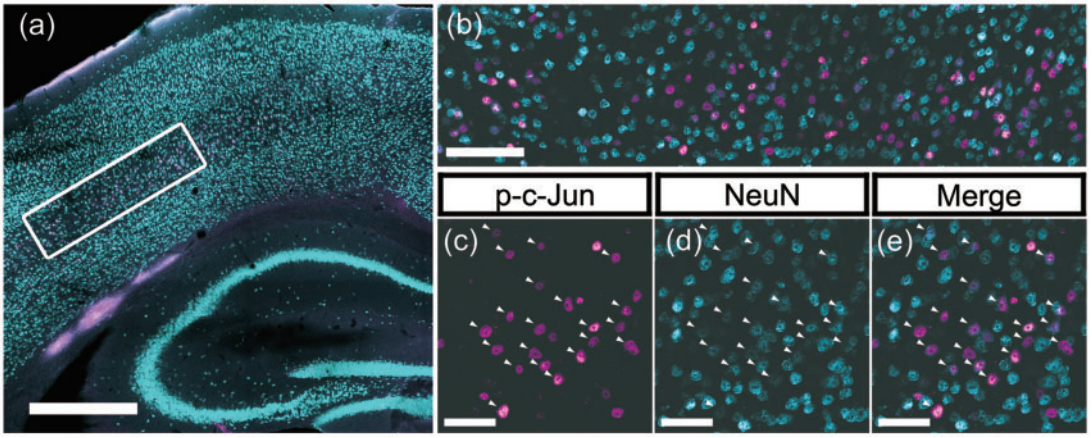

FIGURE 3. Representative immunofluorescent images demonstrating p-c-Jun/NeuN colocalization. Representative immunofluorescent images that underwent quantitative assessments of the burden of diffuse axonal injury in layer V neurons. All presented images originate from the same animal in the HR group and show representative findings after double labeling with p-c-Jun (magenta) and NeuN (cyan), which were used as markers for the axotomized neuronal populations and the total neuron populations, respectively. **(A)** Tiled, 10× magnification image labeling p-c-Jun and NeuN. The white rectangle in the figure presents the location of region of interest (ROI) centering on the layer V neurons. Note that, p-c-Jun signals are distributed primarily in neocortical layer V, consistent with this well-established animal TBI model that generates axotomized neurons in this domain. Scale bar = 500 μm. **(B)** A 20× magnification image of the ROI in neocortical layer V delineated by a white rectangle in panel **(A)**. Fluorescent signals labeling p-c-Jun (magenta) or NeuN (cyan) are distributed broadly in the ROI, showing colocalization. Note, however, that colocalization did not show one to one correspondence. Scale bar = 100 μm. Panels **(C–E)** are enlarged images of one portion of panel **(B)**, in which p-c-Jun and NeuN are presented. Each panel **(C)** and **(D)** presents single channel image for p-c-Jun and NeuN, respectively. Panel **(E)** presents their merged image. Arrowheads indicate the neurons with p-c-Jun and NeuN colocalization. Scale bars = 50 μm.

neuronal nuclear reaction product marked the occurrence of axonal injury in the same labeled neuron.

Quantitative Analysis

Quantification of p-c-Jun+ Distribution Profiles

Using gross microscopic observation in a blinded manner to the samples' identity, p-c-Jun signals were found to be distributed primarily in layer V within neocortex, consistently with our previous study (16). They also were distributed in a limited area of layer II/III in neocortex, and within dentate gyrus of hippocampus and thalamus. The extent of the distribution varied in each sample, most likely linked the burden of axotomy.

The quantitative data of p-c-Jun+ distribution demonstrated the density of p-c-Jun+ neurons after repetitive mTBI, with the higher intensity mild injuries (HR group), generating 478 ± 61 neurons/mm^2 of axotomized neurons (Fig. 5A). This value was significantly different from either the LS or LR groups, but not the HS group (LS; 179 ± 19, LR; 193 ± 53, HS; 241 ± 78 neurons/mm^2. HR vs LS; $d = 3.09$, $p = 0.012$, HR vs LR; $d = 2.11$, $p = 0.017$, HR vs HS; $d = 1.37$, HS vs LS; $d = 0.44$, HS vs LR; $d = 0.29$, LR vs LS; $d = 0.14$). Only injury intensity had a significant main-effect on the differences in the group comparisons (the number of injuries; $\eta^2 = 0.12$, injury intensity; $\eta^2 = 0.28$, $p = 0.010$, and their interaction; $\eta^2 = 0.12$).

Quantification of NeuN+ Distribution Profiles

To estimate the occurrence of axotomy across the total neuron populations and to compare these values among groups, NeuN+ distribution was also quantitatively assessed (Fig. 5B). The density of NeuN+ neurons was LS; 2451 ± 43, LR; 2408 ± 45, HS; 2214 ± 66, and HR; 2237 ± 51 neurons/mm^2, respectively. HS group was significantly different from LS (HR vs LS; $r = 0.69$, HR vs LR; $r = 0.72$, HR vs HS; $r = 0.00$, HS vs LS; $r = 0.84$, $p = 0.045$, HS vs LR; $r = 0.68$, LR vs LS; $r = 0.06$).

Quantification of Colocalization of p-c-Jun and NeuN

Colocalization of p-c-Jun and NeuN was widely observed but was not seen in all p-c-Jun+ neurons. Density of colocalization were LS; 132 ± 18, LR; 130 ± 37, HS; 164 ± 53, and HR; 320 ± 44 cells/mm^2, respectively (Fig. 5C). HR was significantly different from either of LS and LR groups, but not from HS group (HR vs LS; $d = 2.60$, $p = 0.025$, HR vs LR; $d = 2.00$, $p = 0.024$, HR vs HS; $d = 1.31$, HS vs LS; $d = 0.32$, HS vs LR; $d = 0.29$, LR vs LS; $d = 0.02$). Only injury intensity had a significant main-effect on the differences of group comparison (the number of injuries; $\eta^2 = 0.10$, injury intensity; $\eta^2 = 0.25$, $p = 0.018$, and their interaction; $\eta^2 = 0.14$).

The fractions of p-c-Jun+ neurons among whole NeuN expressing neurons were LS; 5.4% (95% confidence interval

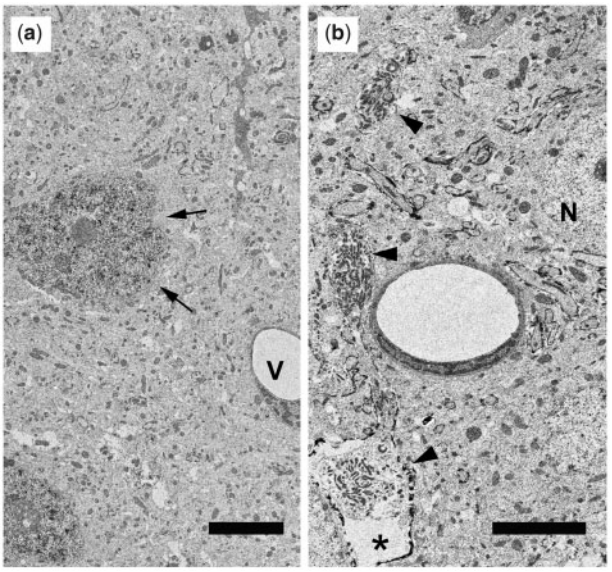

FIGURE 4. Electron micrograph of repetitively injured mouse. **(A)** Electron micrograph taken from a repetitively injured mouse confirms the mild nature of the traumatic injuries. Note that despite the presence of p-c-Jun immunoreactivity within scattered neuronal nuclei (arrows) that reflect the occurrence of axonal injury, the balance of the brain parenchyma is intact, showing normal detail in both its neuronal, glial and vascular (V) constituents. Scale bar = 5 μm. **(B)** Electron micrograph harvested from the same case shown in panel **(A)** again demonstrates the integrity of the brain tissue and its vascular components. Note that a normal/nonreactive neuronal soma (N) can be seen in the field, which also shows a damaged axonal profile (arrowheads) terminating in a reactive axonal swelling (asterisk) all of which represent diffuse axonal injury. Such damaged axons can be traced back to neuronal soma displaying nuclear p-c-Jun. Scale bar = 5 μm.

[95% CI]; 4.6%–6.2%), LR; 5.4% (4.7%–6.2%), HS; 7.4% (6.5%–8.4%), and HR; 14.3% (13.1%–15.6%), respectively (Fig. 5D). The difference in those rates between the 4 groups was significant ($p < 0.001$). In posthoc pairwise comparisons, HR was significantly different from all other groups and HS was significantly different from LS and LR groups, either (HR vs LS; OR = 2.66 [95% CI; 2.22–3.18], $p < 0.001$, HR vs LR; OR = 2.64 [2.20–3.16], $p < 0.001$, HR vs HS; OR = 1.93 [1.63–2.28], $p < 0.001$, HS vs LS; OR = 1.38 (1.13–1.68), $p = 0.007$, HS vs LR; OR = 1.37 [1.12–1.67], $p = 0.007$, LR vs LS; OR = 1.01 [0.81–1.24]). The fraction of NeuN+ neurons among whole p-c-Jun+ expressing neurons (e.g. p-c-Jun/NeuN colocalization within p-c-Jun+ neuron population) were LS; 73.6% (95% CI; 67.6%–79.0%), LR; 67.8% (61.8%–73.4%), HS; 68.0% (62.7%–73.0%), and HR; 66.9% (63.2%–70.5%), respectively (Fig. 5E). There was no significant difference in those rates between groups or in any pairwise comparisons (HR vs LS; OR = 0.91 [95% CI; 0.72–1.14], HR vs LR; OR = 0.99 [0.79–1.24], HR vs HS; OR = 0.98 [0.80–1.21], HS vs LS; OR = 0.92 [0.72–1.19], HS vs LR; OR = 1.00 [0.78–1.29], LR vs LS; OR = 0.92 [0.70–1.21]).

DISCUSSION

The results of this study reveal in a compelling fashion that repetitive mild injury can increase the burden of axonal injury, although this response is a function of injury severity. These findings were highly reproducible and paralleled changes in the proportion of axotomized neurons and the duration of the LORR observed after a single injury; however, there was no increase in the LORR duration following repetitive injury. Collectively, these results support not only the importance of repetitive concussive injuries but also their associated severity. Of equal importance, to our best knowledge, this is the first investigation to model repetitive TBI using cFPI, which reproduces a mild injury and DAI without confounds of overt cell death and/or contusional change in neocortex, which was recently shown to have major implications in circuit disruption in both experimental and clinical mTBI.

Pivotal in our assessment and determination of the burden of axonal damage was the premise that antibodies to p-c-Jun reliantly mapped only to those neuronal soma undergoing DAI within their related axonal segments. This assumption was based upon the longstanding recognition that selective and prolonged expression of c-Jun has been associated with axotomy in both the peripheral and central nervous system (25). While we appreciate that activation of c-Jun, a member of transcription factor, has been thought to play different roles in neuronal cell death, degeneration, gliosis, and inflammation, as well as plasticity and repair (26), we also recognize that, within the context of mTBI, the linkage between phosphorylation of c-Jun and concomitant axotomy has been compelling. In our initial studies (16), we routinely confirmed a precise linkage between axotomy within the layer V projectional neurons and subsequent upregulation of p-c-Jun in the same neuronal population. In parallel studies of mTBI in the visual axis (18), we also observed a compelling correlation between the presence of p-c-Jun upregulation in the retina and axotomy within the optic nerve. Even more compelling evidence for the linkage between these parameters was found in our more recent studies of mTBI (17) in which we closely followed in a subpopulation of neocortical interneurons, the occurrence of DAI in concert with the concomitant expression of p-c-Jun. Utilizing this very discreet interneuronal population, we again confirmed that p-c-Jun expression was a prominently specific, retrograde surrogate marker of DAI. Recently, work from another laboratory has given further credence to the linkage between p-c-Jun expression and axotomy via the use of retrogradely labeled axotomized neurons which were directly mapped to p-c-Jun expression which, in turn, were followed by neuronal atrophic change (19). Thus, within the context of mTBI, there is compelling evidence from multiple fronts that this correlation is valid and provides a viable marker for the detection of axonal change and its quantification. While we cannot unequivocally exclude the potential colocalization of p-c-Jun with other forms of neuronal injury, we must note that neither we nor any other group has provided any evidence that this is the case.

As reported, our current data revealed a significantly higher proportion of p-c-Jun+ neurons after repetitive mild in-

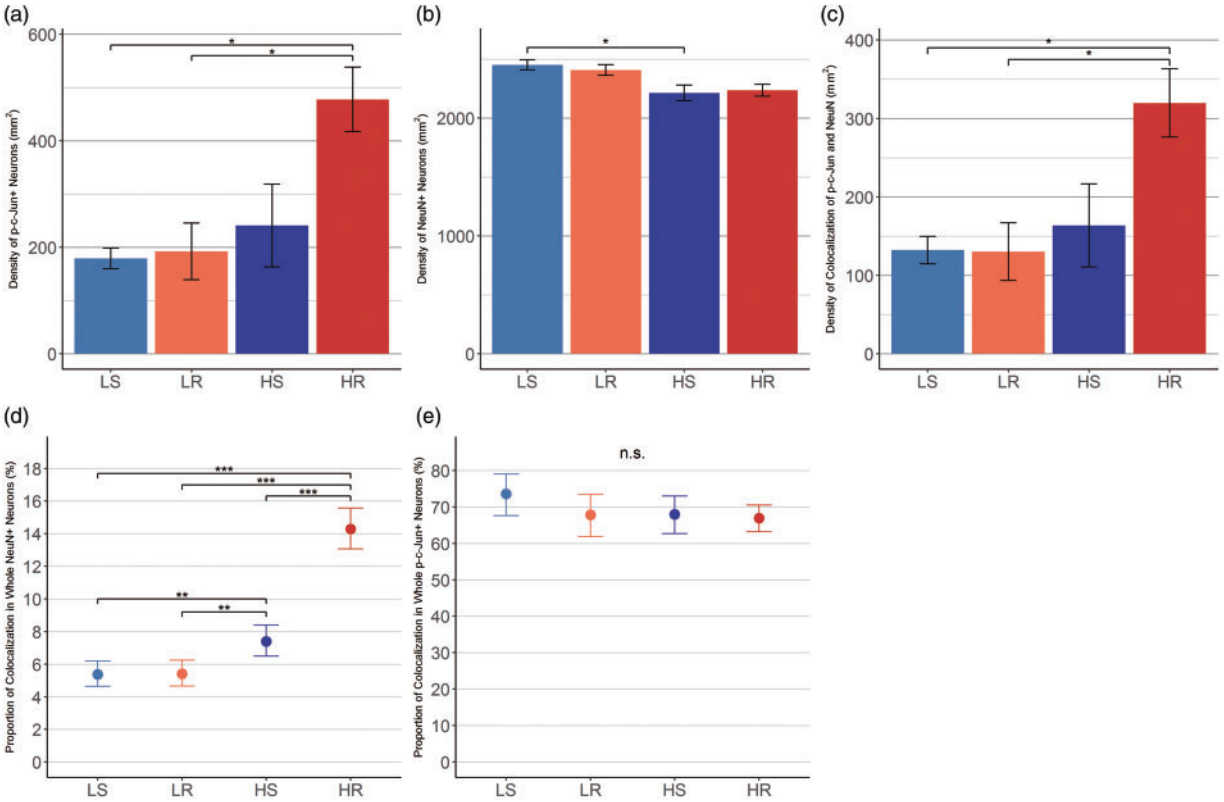

FIGURE 5. Quantitative assessment of p-c-Jun+/NeuN+ neurons. Quantitative assessments of p-c-Jun+/NeuN+ neurons. **(A)** The density of p-c-Jun+ neurons in the ROI. HR group demonstrated significant difference compared with LS and LR groups, but not to HS group (vs LS; $d = 3.09$, $p = 0.012$. vs LR; $d = 2.11$, $p = 0.017$. vs HS; $d = 1.37$, $p = 0.0528$). **(B)** The density of NeuN+ neurons in the same ROI. Significant difference was observed in comparison between HS and LS groups ($r = 0.84$, $p = 0.045$). **(C)** The density of p-c-Jun/NeuN colocalization. HR group demonstrated significant difference compared with LS and LR groups, but not to HS group (vs LS; $d = 2.60$, $p = 0.025$. vs LR; $d = 2.00$, $p = 0.024$. vs HS; $d = 1.31$, $p = 0.071$). **(D)** The proportions of p-c-Jun/NeuN colocalization in the total NeuN+ neuron population. Estimated proportion of axotomy was 14.3% (95% CI; 13.1%–15.6%) in HR group, 7.4% (95% CI; 6.5%–8.4%) in HS, and they were significantly different. The OR of HR group to HS was 1.93 (95% CI; 1.63–2.28). In contrast, LR and LS group did not show significant difference and the OR was 1.01 (95% CI; 0.81–1.24). **(E)** The proportion of p-c-Jun/NeuN colocalization within p-c-Jun+ neuron population. Approximately 70% of p-c-Jun+ neurons were positive for NeuN. There was no difference between the groups. Error bars indicate the standard error of the means in **(A–C)** and 95% CI of the estimated proportions in **(D)** and **(E)**. Pairwise comparisons were assessed by Tukey's HSD test in **(A–C)**, and by Chi-square test followed by pairwise Chi-square test with Holm's correction in **(D)** and **(E)**. *d*; Cohen's *d* with Hedges correction, *r*; effect size for comparison of nonparametric variables, 95% CI; 95% confidence interval. *$p < 0.05$, **$p < 0.01$, ***$p < 0.001$, n.s.; not significant. LS; lower intensity single mild injury, LR; lower intensity repetitive mild injury, HS; higher intensity single mild injury, HR; higher intensity repetitive mild injury.

juries of higher intensity compared with singular injuries or the lower intensity repetitive injuries. Among the pairwise comparisons of the proportion of axotomized neurons between repetitive and single injury of the same injury intensity, a difference was only observed between HR and HS accompanied by an OR of 1.93, but not between LR and LS (OR = 1.01). These results clearly demonstrated that mTBIs of different injury intensities differently impact the burden of DAI. Though we failed to demonstrate such significant differences in the density of p-c-Jun+ neurons (Fig. 5A) and in their colocalization with NeuN (Fig. 5C), the pairwise comparisons within higher intensity groups (e.g. HR vs HS) demonstrated a large effect size of the repetitive insult which was much higher than that within the lower intensity groups (e.g. LR vs LS). Further, this was also supported by the analyses using two-way ANOVA demonstrating the injury intensity as the main effect in determining the burden of DAI. We previously reported that the injury severity, together with the duration interval between insults, is an important variable in the context of the cerebral vascular response to TBI (14) with the suggestion that this was also the case for brainstem DAI identified through amyloid precursor protein immunostaining. In concert with these studies, the current report clearly demonstrates the importance of injury severity for influencing the total burden of DAI.

The density of NeuN+ neurons was significantly decreased in the HS group compared with LS group, and large effect size was demonstrated, in addition to this combination, in the pairs of HR and LS groups, HR and LR groups, and HS and LR groups. However, despite these data suggesting

NeuN+ neuron reduction, our EM findings did not reveal any evidence of increased neuronal death in higher intensity or repetitive injury groups, consistent with our previous reports that our model does not result in neuronal death (16, 17). It has been recently recognized that the expression of NeuN may vary in its distribution and the intensity depending on neuronal type and pathological condition (27). Taking these factors together, we speculate the observation in the density of NeuN+ neurons in the current communication did not reflect neuronal death. Rather, it suggests an alteration of NeuN expression in some axotomized neurons, a premise that requires further in-depth investigation.

The length of the chosen interval between 2 insults explored in this study was 3 hours and this choice was based on previous studies which demonstrated that this interval was adequate to evoke exacerbated vascular dysfunction, which was reduced if the interval was extended to 5 hours and eliminated with an interval of 10 hours (14). While this interval may not be directly relevant to human repetitive TBI, it did generate consistent axonal damage. As it is well recognized that the time frame for rodent repetitive TBI may not approximate that found in humans, we believe that our findings remain meaningful. Obviously, future studies in other models of injury and in different species will be required to confirm our reported axonal vulnerability.

The LORR is a widely used measure for assessing the loss of consciousness in animals (22), which also reflects the severity of employed injury in the cFPI model (21). We consistently demonstrated that higher intensity single mild injuries caused significantly longer LORR compared with lower intensity single mild injuries (Fig. 2A). Noteworthy was the fact that both HR and LR groups did not show any significant difference between the first LORR and the second LORR, suggesting that the LORR is certainly an accurate measure of injury severity with single mTBI, but is not the case after repetitive mTBI. The reasons for this are unknown; however, it is possible that, with mTBI, a threshold of LORR may present.

There were several limitations in the current study. There were unexpected differences in respiratory rates observed during the surgical preparation between groups, although all other physiological features were similar and within normal limits. Reviewing all data, we recognized that those animals obtained directly from the commercial supplier revealed lower respiratory rates compared with those mice bred in our laboratory. As all animals had the same genetic background, we remain puzzled by this observation, however, in future studies, we will avoid a mixture of mouse sources to improve rigor and reproducibility. There was also a difference in the duration over which the animals were under anesthesia. However, given that all other physiological variables were within normal limits and considerable recovery time after anesthesia was maintained before the first injury for all animals, it is not likely that this could have significantly impacted on this study. Of additional concern was the finding that only 70% of p-c-Jun positive neurons were colocalized with NeuN (Fig. 5). Recognizing from our previous study (16) that non-neuronal cells expressing p-c-Jun are rare, we speculate that this observed mismatch was most likely linked to the technical limitations of our current study and/or the biological heterogeneity of DAI. We cannot, however, discount the possibility that some axotomized neurons did not express NeuN, in light of the possible parallel alterations in NeuN expression induced by the pathological event.

The burden of DAI after repetitive mTBI was exacerbated by the increase of injury intensity, while the second LORR of repetitively injured animals was not prolonged by the second injury regardless of its severity. These contrasting results directly suggest that the injury intensity of mTBI is an important variable to determine pathological severity in respect of neocortical DAI, not accompanied by the alteration of LORR, which may be the sole symptom of mTBI. These current findings contribute not only to our better understanding of the differences between single and repetitive mTBI but also to the design of future studies to explore those pathologies occurring with repetitive mTBI.

ACKNOWLEDGMENT

The authors thank Carol Davis and Susan Walker for their invaluable technical assistance. Scott Henderson and Frances White for sharing their expertise in confocal microscopy. Robert J. Hamm for expert advice on statistics. Audrey Lafrenaye, Vishal Patel for their scientific insights and advice.

REFERENCES

1. Cassidy JD, Carroll LJ, Peloso PM, et al. Incidence, risk factors and prevention of mild traumatic brain injury: Results of the WHO Collaborating Centre Task Force on mild traumatic brain injury. J Rehabil Med 2004;36:28–60
2. Mortimer JA, Van Duijn CM, Chandra V, et al. Head trauma as a risk factor for Alzheimer's disease: A collaborative re-analysis of case-control studies. Int J Epidemiol 1991;20:S28–35
3. Fleminger S, Oliver DL, Lovestone S, et al. Head injury as a risk factor for Alzheimer's disease: The evidence 10 years on; a partial replication. J Neurol Neurosurg Psychiatry 2003;74:857–62
4. Chen H, Richard M, Sandler DP, et al. Head injury and amyotrophic lateral sclerosis. Am J Epidemiol 2007;166:810–6
5. Jafari S, Etminan M, Aminzadeh F, et al. Head injury and risk of Parkinson disease: A systematic review and meta-analysis. Mov Disord 2013; 28:1222–9
6. McKee AC, Cantu RC, Nowinski CJ, et al. Chronic traumatic encephalopathy in athletes: Progressive tauopathy after repetitive head injury. J Neuropathol Exp Neurol 2009;68:709–35
7. Laurer HL, Bareyre FM, Lee VMYC, et al. Mild head injury increasing the brain's vulnerability to a second concussive impact. J Neurosurg 2001;95:859–70
8. Raghupathi R, Mehr MF, Helfaer MA, et al. Traumatic axonal injury is exacerbated following repetitive closed head injury in the neonatal pig. J Neurotrauma 2004;21:307–16
9. Longhi L, Saatman KE, Fujimoto S, et al. Temporal window of vulnerability to repetitive experimental concussive brain injury. Neurosurgery 2005;56:364–73
10. Huh JW, Widing AG, Raghupathi R. Repetitive mild non-contusive brain trauma in immature rats exacerbates traumatic axonal injury and axonal Calpain activation: A preliminary report. J Neurotrauma 2007;24:15–27
11. Friess SH, Ichord RN, Ralston J, et al. Repeated traumatic brain injury affects composite cognitive function in piglets. J Neurotrauma 2009;26: 1111–21
12. Prins ML, Hales A, Reger M, et al. Repeat traumatic brain injury in the juvenile rat is associated with increased axonal injury and cognitive impairments. Dev Neurosci 2010;32:510–8

13. Shitaka Y, Tran HT, Bennett RE, et al. Repetitive closed-skull traumatic brain injury in mice causes persistent multifocal axonal injury and microglial reactivity. J Neuropathol Exp Neurol 2011;70:551–67
14. Fujita M, Wei EP, Povlishock JT. Intensity- and interval-specific repetitive traumatic brain injury can evoke both axonal and microvascular damage. J Neurotrauma 2012;29:2172–80
15. Smith DH, Hicks R, Povlishock JT. Therapy development for diffuse axonal injury. J Neurotrauma 2013;30:307–23
16. Greer JE, McGinn MJ, Povlishock JT. Diffuse traumatic axonal injury in the mouse induces atrophy, c-Jun activation, and axonal outgrowth in the axotomized neuronal population. J Neurosci 2011;31: 5089–105
17. Vascak M, Jin X, Jacobs KM, et al. Mild traumatic brain injury induces structural and functional disconnection of local neocortical inhibitory networks via parvalbumin interneuron diffuse axonal injury. Cereb Cortex 2018;28:1625–44
18. Wang J, Fox MA, Povlishock JT. Diffuse traumatic axonal injury in the optic nerve does not elicit retinal ganglion cell loss. J Neuropathol Exp Neurol 2013;72:768–81
19. Ziogas NK, Koliatsos VE. Primary traumatic axonopathy in mice subjected to impact acceleration: A reappraisal of pathology and mechanisms with high-resolution anatomical methods. J Neurosci 2018;38: 2343–17
20. Vascak M, Sun J, Baer M, et al. Mild traumatic brain injury evokes pyramidal neuron axon initial segment plasticity and diffuse presynaptic inhibitory terminal loss. Front Cell Neurosci 2017;11:1–24
21. Dixon CE, Lyeth BG, Povlishock JT, et al. A fluid percussion model of experimental brain injury in the rat. J Neurosurg 1987;67:110–9
22. Meyer RE, Euthanasia and humane killing. In: Grimm KA, Lamont LA, Tranquilli WJ, et al. eds. Veterinary Anesthesia and Analgesia: The Fifth Edition of Lumb and Jones. Hoboken, NJ: John Wiley & Sons, Inc. 2015: 130–43
23. Hånell A, Greer JE, McGinn MJ, et al. Traumatic brain injury-induced axonal phenotypes react differently to treatment. Acta Neuropathol 2015;129:317–32
24. Stone JR, Walker SA, Povlishock JT. The visualization of a new class of traumatically injured axons through the use of a modified method of microwave antigen retrieval. Acta Neuropathol 1999;97:335–45
25. Hughes PE, Alexi T, Walton M, et al. Activity and injury-dependent expression of inducible transcription factors, growth factors and apoptosis related genes within the central nervous system. Prog Neurobiol 1999; 57:421–50
26. Raivich G. c-Jun Expression, activation and function in neural cell death, inflammation and repair. J Neurochem 2008;107:898–906
27. Duan W, Zhang YP, Hou Z, et al. Novel insights into NeuN: From neuronal marker to splicing regulator. Mol Neurobiol 2016;53:1637–47